REAL-TIME TEST OF MOCS ALGORITHM

DURING SUPERFLUX 1980

Gary W. Grew
NASA Langley Research Center

SUMMARY

During the October Superflux experiments a remote sensing experiment was conducted in which success depended upon the real-time use of a new algorithm, generated from MOCS (Multichannel Ocean Color Sensor) data onboard the NASA P-3 aircraft, to direct the NOAA ship Kelez to oceanic stations where vitally needed sea truth could be collected. Remote data sets collected on 2 consecutive days of the mission were consistent with the sea truth for low concentrations of chlorophyll a. Two oceanic regions of special interest were located and are being analyzed.

INTRODUCTION

As plans for the Superflux experiments were taking shape, a new ocean color algorithm for remotely monitoring suspended solids was under investigation. The algorithm is the outcome of analyses of remote data collected over a 6-year period with MOCS (Multichannel Ocean Color Sensor). Most of the MOCS data were collected in nearshore regions over plumes consisting of complex mixtures of suspended solids. To verify the potential of the algorithm, data was needed from offshore regions away from the high turbidity waters in the coastal zone. In particular, data was needed over deep water where chlorophyll a concentrations vary between 0.1 to 10 $\mu g/\ell$. The expected participation in the Superflux experiments of the NOAA ship Kelez, with its capability of collecting sea truth data offshore and analyzing water samples onboard, offered an excellent opportunity for obtaining the vitally needed data to verify the algorithm.

The Superflux experiments also presented an opportunity for demonstrating the potential of the MOCS-aircraft real-time ocean color analyzer system. This system was developed for directing ships to positions where sea truth could be collected during the overflights. On past missions in which there was little or no foreknowledge of the compositions and concentrations of the suspended solids in the region of study, sea truth data were generally collected at evenly spaced points along flight tracks. The degree of success in obtaining the needed sea truth by this hit or miss technique has not been high. One purpose of this paper is to show that mission success can be greatly improved with the MOCS real-time system, which relies on the new algorithm for interpreting the color of the ocean.

MOCS-AIRCRAFT REAL TIME OCEAN COLOR ANALYZER (MARTOCA)

There are two basic parts to the MARTOCA system: the MOCS itself and the data processing subsystem. MOCS is a visible imaging spectroradiometer which performs multispectral scanning electronically by means of an image dissector (ref. 1). It covers the visible region of the spectrum, 400 to 700 nanometers, in 20 adjacent bands (tables 1 and 2). As shown in figure 1, the output from MOCS is fed into an A/D converter; all the data is stored serially on an analog tape recorder.

By means of the data selector in the real-time subsystem, samples of the data, usually center-of-track data, are processed and stored in a microprocessor; this data can be stored in and recalled from a digital tape recorder. During flight, or in the laboratory, a thumb wheel algorithm selector is used to display on an x-y oscilloscope cross plots of the algorithm or plots of the algorithm versus distance along the flight track. An example of the x-y display is presented in this paper.

In a much improved version of the real-time system currently under development, Loran C data will be fed into a minicomputer along with MOCS data. With this system latitude and longitude positions of special oceanic features can be determined rapidly and accurately.

ALGORITHM

Background

The algorithm is an outcome of the investigation of MOCS data by means of characteristic vector analysis (ref. 2). The data collected over Chesapeake Bay plumes reveal specific eigenvectors associated with specific regions on both sides of major plume boundaries. These eigenvectors have characteristic features which consistently appear, but their relative magnitudes vary due to interfering environmental factors, such as solar elevation, cloud cover, and sea state. One often-neglected variable is ocean surface reflection which can vary significantly across boundaries separating different water masses. MOCS data in conjunction with sea truth demonstrate that magnitude variations in the upwelling light due to such environmental changes can be much larger than the signal variations resulting from different algae concentrations. To show the effects of the environmental factors on spectral features and to simplify the discussion of the basis for the algorithm, comparisons between two pairs of MOCS spectra are presented.

In figure 2 the first pair of raw MOCS data was collected 2 nautical miles apart across a Chesapeake Bay plume boundary. Most of the signal variation between the two spectra seems to be due to algae concentration. If so, the plot in figure 3 of the differences in percent of these spectra shows features associated with the absorption and scattering properties of algae. For example, the chlorophyll a absorption band in the red region of the spectrum (675 nm) is evident about band 19. If no other factors influenced the upwelling

light, such difference spectra could be used to identify and map algae. Finding such pairs of spectra, however, is the exception rather than the rule.

A more typical case can be demonstrated with the spectra in figure 4 collected on different days under different environments for low and high concentrations of chlorophyll a. The large magnitude differences in the two spectra in figure 4(a) are a result of environmental factors, not the algae. The two spectra are shown normalized in figure 4(b) to illustrate, as in figure 3, the small differences in the spectral shapes. In figure 5, the difference spectra for this pair have features similar to those in figure 3 but distorted by environmental factors. Analyses of other MOCS data have shown that environmental parameters distort spectral signatures of suspended solids unequally across the visible spectrum, the variation being greater in the red region of the spectrum than in the blue. Since these variations will cause simple ratios of spectral bands, as well as single band data, to vary with environmental changes, it is difficult, if not impossible, to use these ratios to remotely quantify suspended matter in the ocean without extensive sea truth. An algorithm is needed which monitors only the significant information in each spectrum, e.g., for one particular region, the information within the envelope defined by the spectral differences in figure 3.

Equation

The consistency of spectral features, such as those in figure 3, in conjunction with the problems associated with the environmental factors led the author to investigate the algorithm

$$
G_{j,m,n} = \frac{(S_j)^2}{S_{(j-m)} \cdot S_{(j+n)}} \tag{1}
$$

where S_j is the MOCS signal for band j and m and n are constants. This algorithm, which amplifies and monitors changes in the spectral features, has been labeled "inflection ratio algorithm."

The rationale for this algorithm is based on the principle that at least three points are required to define a spectral feature. Consider the chlorophyll a absorption band in figure 3 that can be defined by bands 17, 19, and 20. A number of algorithms using three bands are, of course, possible, but such algorithms as

$$S_{17} + S_{19} + S_{20}$$

and

$$S_{17} \bullet S_{19} \bullet S_{20}$$

vary with the environment. Analyses of MOCS data have shown that, while simple ratios such as

$$\frac{S_{19}}{S_{17}} \quad \text{and} \quad \frac{S_{20}}{S_{19}}$$

vary with the environment, the ratio of the two ratios varies significantly less. Thus,

$$\frac{\dfrac{S_{19}}{S_{17}}}{\dfrac{S_{20}}{S_{19}}} = \frac{S_{19}}{S_{17}} \bullet \frac{S_{19}}{S_{20}} \tag{2}$$

$$= \frac{(S_{19})^2}{S_{17} \bullet S_{20}} \tag{3}$$

which by equation (1) is equal to $G_{19,2,1}$

As a first step toward simplifying the analyses, the author investigated all forms of the $G_{j,m,n}$ algorithm in which m equals n or

$$G_{j,m} = \frac{(S_j)^2}{S_{j-m} \bullet S_{j+m}} \tag{4}$$

Subsequently, as a further simplification, all possible values of this algorithm for $m = 2$, or

$$G_{j,2} = \frac{(S_j)^2}{S_{j-2} \bullet S_{j+2}} \qquad j = 3\text{--}18 \tag{5}$$

304

were investigated because (1) the smaller the value of m the less the influence of the environment on the algorithm, and (2) the spectral features have half-widths of about 30 nanometers or greater.

Inflection ratio spectra for m = 2 derived from MOCS spectra collected over relatively clear water on various missions are shown in figure 6. The atmospheric and sea conditions varied from mission to mission and the solar elevation angle during each overflight varied widely, as indicated in the figure. Since these curves are very consistent, one can be selected as a standard for examining the relative changes in the inflection ratio spectra for different water masses through the equation

$$H_{j,2} = \left(\frac{G_{j,2}}{G_{j,2}(\text{standard})} - 1 \right) 100 \quad j = 3\text{--}18 \tag{6}$$

Plots of $H_{j,2}$ for the two MOCS spectra in figure 4 are shown in figure 7. By comparing figure 7 with figure 5 (or fig. 3) features in the inflection ratio spectrum of high chlorophyll a concentration can be associated with the spectral features of algae. This inflection ratio spectrum consistently can be generated from MOCS data collected over strong algae plumes. While the corresponding difference spectra, as in figure 5, could vary drastically for data collected over the same algae concentrations but under different environments, the inflection ratio spectra appear to remain relatively constant.

A second type of inflection ratio spectrum, often appearing but not clearly identified, is shown in figure 8. Indirect evidence, however, prior to the Superflux experiments suggested this spectrum may be associated with organic detritus. Evidence supporting this possibility is presented in later paragraphs.

OCTOBER MISSION

Operations

Because of several factors, the weather in particular, the goal of the MOCS experiment of collecting deep ocean data along with adequate sea truth was not met during the spring and summer Superflux experiments. Thus, for the October mission a plan was formulated for increasing the probability of mission success and at the same time for demonstrating the real time capability of the MOCS system.

The basic plan consisted of 2 consecutive days of MOCS data collection missions from an aircraft altitude of 2.3 km. An exploratory mission would be conducted on the first day with or without sea truth collection. The P-3 aircraft would be directed to fly out to and along the shelf break in search of a region where, based on the MOCS algorithm, a definite chlorophyll a concentration gradient existed across a boundary separating two different water

masses. If such a region were located, the NOAA ship Kelez would be directed to collect sea truth data in that region during the overflights on the second day.

Due to airway restrictions during the experiment the P-3 flights were confined to a narrow corridor between latitudes 36°55' N and 37°2' N. Fortunately our first flight track along latitude 36°56' N resulted in data collection over several different water masses including the desired chlorophyll a gradient. In addition, the experiment was fortunate enough to have the Kelez available to collect sea truth on both days.

The mission began at 1:00 a.m. on October 21, 1980, when the Kelez collected the first of a series of water bucket samples as it steamed toward the end of the track, shown in figure 9, to await the P-3 overflights. By 8:53 a.m. when the P-3 began its overflight along the same track, the Kelez was stationed at 36°56' N, 74°20' W. Using the MOCS algorithm a well-defined boundary was located near longitude 74°40'. No visible boundary was observed at the time by either the P-3 or the Kelez, nor was it observable later on aerial photography. Based on this boundary the Kelez was directed to collect additional sea truth data along the same track between 74°20' and 74°50' and then to remain in the region for the P-3 overflights the next day.

On the second day the Kelez again collected sea truth between the same coordinates during the P-3 overflights. In addition, the Kelez was directed to collect data at three specific locations on its return transit to port. Based on the MOCS algorithm each of these locations was in a different water mass.

Prediction

One of the x-y oscilloscope displays used in the real time analysis of ocean color is the cross plot of $G_{7,2}$ and $G_{12,2}$ for data along the center of the track. Figure 10 shows data collected from an altitude of 2.3 km on the first overflight (fig. 9) on October 21, 1980. Each point in the figure is equivalent to one data sample with a spacial resolution of 50 meters collected about every 300 meters along the track. Patterns similar to the one in the figure have been obtained on other missions. The same unnormalized scales are always used. Based on the large number of similar plots and their corresponding sea truth, this plot was interpreted in real time as stated below.

There appeared to be four basic oceanic regions, as labeled in figure 11, corresponding to four different types of water masses. Region 1, located east of the shelf break, consisted of very clear water with chlorophyll a concentrations less than 1 µg/l. Region 2 west of the shelf break had higher chlorophyll a than Region 1 but the average concentration was probably less than 2 µg/l. This is verified by examining the plot of the change in the inflection ratio spectra between Regions 1 and 2, as shown in figure 12. Spectra are shown for both days of the mission, as well as for a similar condition observed during the June mission. The prominent feature in the blue region of the spectrum was caused by a change in the absorption of light by phytoplankton across the shelf break, clearly indicating a phytoplankton gradient existed there.

Region 3 indicated that the average chlorophyll $\underline{a}$ was lower than in Region 2 but the turbidity was higher. The inflection ratio spectra between Regions 2 and 3 are shown for both days in figure 13. The shapes of these curves are characteristic of spectra from regions suspected of consisting of organic detritus (compare fig. 8 and fig. 13). It is possible that Region 3 could be an organic detritus plume.

Region 4 was considered to be the Chesapeake Bay plume. In this paper only regions outside the plume will be discussed, that is, Regions 1 to 3.

It was this real time analysis that led to directing the Kelez to collect sea truth data across the shelf break and in Region 3 on its return to port.

Sea Truth

Sea truth measurements from 37 bucket samples collected by the Kelez on a transit out to the shelf break on October 21, 1980, are shown in figure 14. Chlorophyll $\underline{a}$ concentration and F_o/F_a are plotted versus longitude position along latitude 36°56'. The F_o/F_a index is a linear function of the ratio of pheopigment to chlorophyll plus pheopigment in which a value of 1.1 indicates mainly pheopigment and 2.0 indicates mainly chlorophyll (ref. 3). Since by figure 12 $G_{7,2}$ is the most responsive algorithm to the data in Regions 1 and 2, it is used in figure 14 for comparison with the sea truth; $G'_{7,2}$, the inverse of $G_{7,2}$, is actually plotted to show a positive correlation with the sea truth.

In agreement with $G'_{7,2}$ four fairly distinct regions are evident by the chlorophyll $\underline{a}$ data--assuming that the transitions between regions are not considered to be regions. By visual inspection $G'_{7,2}$ and chlorophyll $\underline{a}$ appear to correlate well in Regions 1 and 2. In Region 3 $G'_{7,2}$ seems to correlate better with F_o/F_a.

Chlorophyll $\underline{a}$

The cross plot of $G_{7,2}$ and chlorophyll $\underline{a}$ in figure 15 indicates a nonlinear relationship exists between the two parameters. A curve similar to Duntley's plot in figure 16 of reflectance for $\lambda = 450$ nm versus chlorophyll $\underline{a}$ was in fact expected. The scatter in the data for Regions 3 and 4 may be due partly to the time difference of 6 to 8 hours between water bucket collection and the overflight. However, the shape differences in the plots (fig. 14) for Region 3 suggest that the apparent scatter may be caused by the mixture of suspended substances in that region.

Figure 17 shows consistent chlorophyll a data in Regions 1 and 2 for both days of the experiment. This data set is the first good set from MOCS to be used in establishing a data base for remote sensing of low chlorophyll a concentrations. In figure 18 the author has taken the liberty of adding to the data set the average of the four data points for Region 4 and using it to draw a dashed curve similar to Duntley's plot (fig. 16). There is evidence, however, to suggest that the curve would not level off as quickly for high concentrations of chlorophyll a away from turbid coastal waters. Future missions being planned or proposed will be directed toward establishing the correct curve.

<center>F_o/F_a Ratio</center>

An investigation is being conducted to determine the significance of the similarities in the shapes of the curves for $G'_{7,2}$ and F_o/F_a in Region 3 (fig. 14). The cross plot of these two parameters in figure 19 shows that, while possible linear curves could be drawn between subsets of points, a complex pattern exists for the whole data set. This plot demonstrates, as should be expected, that different mixtures of suspended solids will influence an algorithm differently.

A variation of the $G_{7,2}$ algorithm was found that correlates fairly well with F_o/F_a for the three regions on the shelf (Regions 2 to 4). This algorithm is given by

$$G_{7,3,2} = \frac{S_7^{\ 2}}{S_4 \circ S_9} \tag{7}$$

where band 5 has been replaced with band 4. Figure 20 shows two plots of this algorithm, one for each day of the mission. Even though the sea truth was collected 24 to 36 hours before the MOCS data for the second day, a linear relationship is evident in both cases. The data loop in the upper left corner of the figure indicates that the MOCS data and sea truth are out of phase; in other words the "plume" had shifted from one day to the next. To show this more clearly, the algorithm and the inverse of F_o/F_a are plotted versus sea truth station in figure 21. Based on this algorithm the plume shifted eastward. The relative magnitudes of the "plume" for the 2 days are uncertain because of a shift in the algorithm, and one of the two data points collected by the Kelez near this region on its return to port does not seem to agree with this shift. Further analysis may clear up this uncertainty.

This "plume" is interesting from several aspects. The F_o/F_a ratio has been used by marine biologists as an indicator of grazing regions of zooplankton. These tiny animals eat phytoplankton converting chlorophyll a into

pheopigments. Thus, low values of F_o/F_a such as in Region 3 (fig. 14), may indicate a depletion of algae by ingestion.

It is also possible the region is associated with either an old algae plume from the Chesapeake Bay or with resuspended solids high in organic matter. In these cases low values of F_o/F_a may indicate the presence of organic detritus. It is reasonable to expect the F_o/F_a index, the color of the ocean and, therefore, the inflection ratio spectrum to vary with the percentage of live and dead algae in the ocean. There is evidence suggesting that similar regions existed beyond the Chesapeake Bay plumes during both the spring and summer Superflux experiments, but the sea truth data analyzed thus far has not been sufficient for understanding this region.

One fact is quite clear, however: the inflection ratio spectra (fig. 13) from this region are distinctly different from those of algae (fig. 7). A dedicated experiment is needed to remotely locate this region and then to collect water samples for thorough analyses of the constituents in the water.

CONCLUDING REMARKS

The October mission was the most successful MOCS experiment conducted to date, primarily because of the real-time connection between the remote sensor on the aircraft and the sea truth ship. Predictions based on the real-time analysis of the MOCS algorithm were used to direct the Kelez to specific sea truth stations. The goal of locating a prime region of interest was achieved along with the successful collection of in situ data in that region. The data sets consisting of remote and in situ data for both days were consistent. It is anticipated that this data will play an important role in testing algorithmic consistency of future data sets of low concentrations of chlorophyll a. Real time predictions during the mission based on the algorithm were, as a whole, confirmed by the sea truth data.

The mission was also successful in that an additional oceanic region was located which may be of fundamental interest to marine biologists. Although the sea truth data presently available is not adequate to "explain" this region (Region 3 in fig. 14), discovery of it and its remote sensing signature may have set the stage for future experiments concerning its nature.

Analysis of the MOCS data with the sea truth, in addition to confirming predictions and demonstrating data consistency, reaffirmed the author's conviction concerning a fundamental point: no one j value of the MOCS algorithm or of any other simple algorithm is likely to be found that can be used alone to quantify different kinds of suspended matter. As supported by the plots in figures 15 and 19, different mixes influence the color of the ocean differently. In low turbidity water offshore $G_{7,2}$ (or $G_{7,3,2}$) and $G_{12,2}$ may be adequate, but MOCS data from other experiments suggest that perhaps as many as eight j values of $G_{j,2}$ may be required to identify and accurately quantify nearshore plumes.

REFERENCES

1. White, P. G.; Jenkin, K. R.; Ramsey, R. C.; and Sorkin, M.: Development and Flight Test of the Multichannel Ocean Color Sensor (MOCS). NASA CR-2311, 1973.

2. Grew, G. W.: Characteristic Vector Analysis as a Technique for Signature Extraction of Remote Ocean Color Data. Remote Sensing of Earth Resources, vol. VI, F. Shahrokhi, ed., The University of Tennessee Space Institute (Tullahoma), 1977, pp. 109-144.

3. Walsh, J. J.; Whitledge, T. S.; Barvenick, F. W.; Wirick, C. D.; Howe, S. D.; Esais, W. E.; and Scott, J. T.: Wind Events and Food Chain Dynamics Within the New York Bight. Limnology and Oceanography, vol. 23, no. 4, 1978, pp. 659-683.

4. Duntley, S. Q.: Detection of Ocean Chlorophyll From Earth Orbit. Fourth Annual Earth Resources Program Review, vol. IV, MSC-05937, 1972.

TABLE 1.- MOCS SPECIFICATIONS

Sensor:	Image Dissector
Scan Rate:	3.51 Scans/sec.
Number of Spectra:	150 Spectra/Scan
Spectral Range:	400-700 nm (Table 2)
Spectral Resolution:	15 nm
Field-of-View:	17.1°
Spacial Resolution:	4 x 2 millirad.

TABLE 2.- MOCS SPECTRAL BANDS

Band	Center Wavelength (nanometers)	Band	Center Wavelength (nanometers)
1	400	11	552
2	415	12	568
3	430	13	584
4	445	14	601
5	460	15	616
6	475	16	631
7	490	17	647
8	506	18	663
9	521	19	678
10	537	20	694
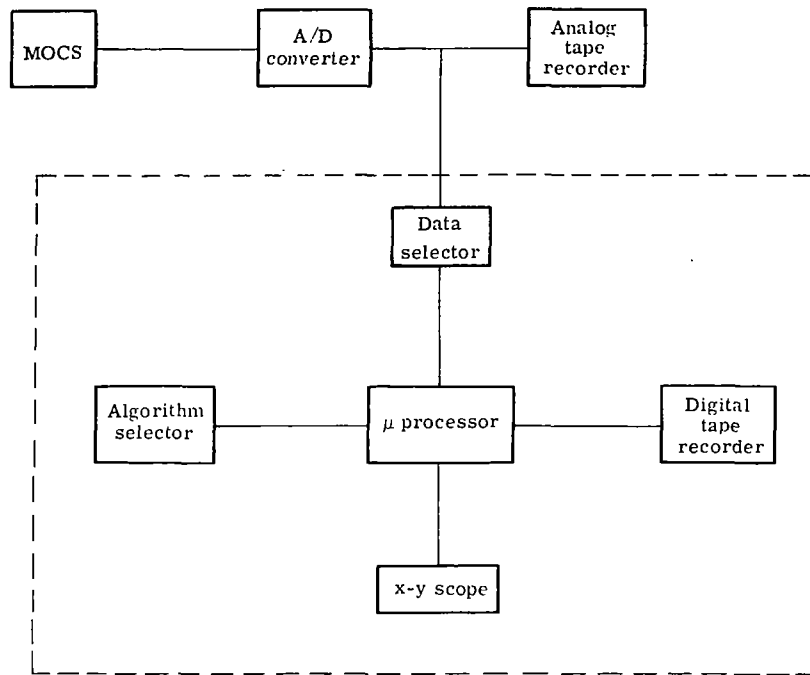
Figure 1.- MOCS aircraft real-time ocean color analyzer.
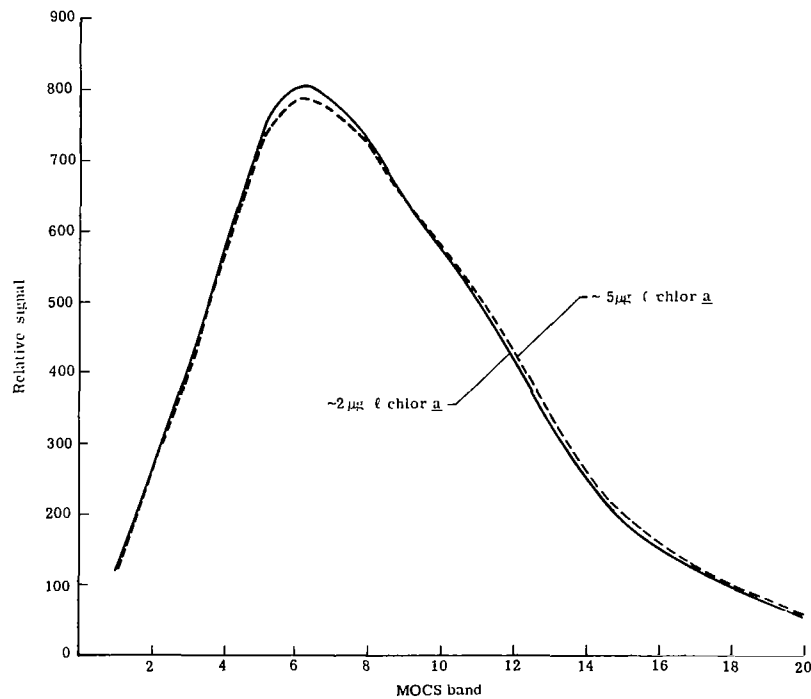
Figure 2.- Raw MOCS spectra collected on April 7, 1976 from 5.3 km altitude near Chesapeake Bay entrance.
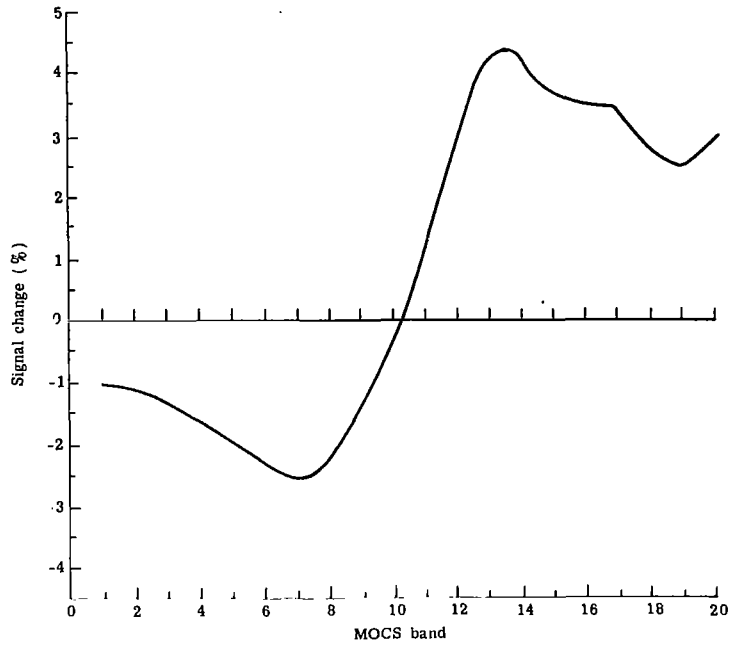
Figure 3.- Difference spectra of 2-5 µg/ℓ chlorophyll a̱ from figure 2.
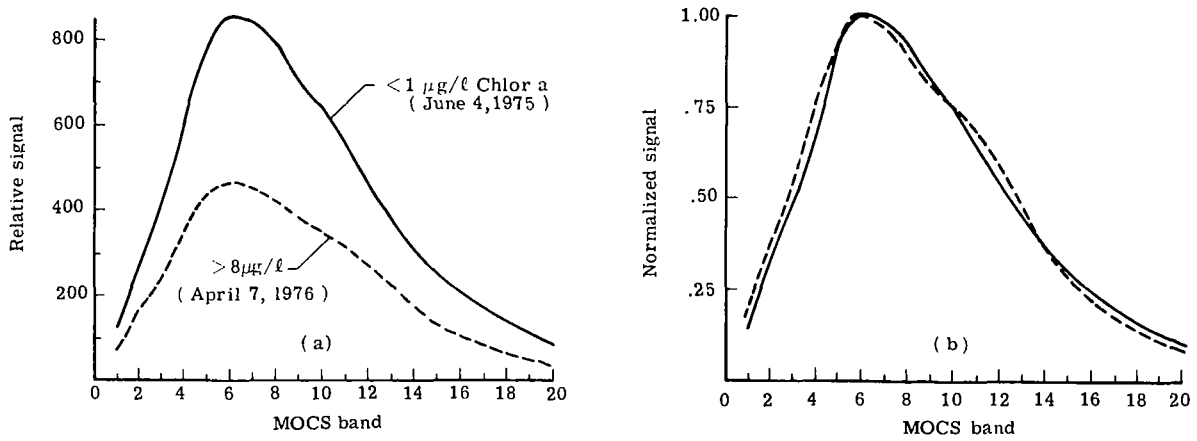
Figure 4.- Raw MOCS spectra (normalized in (b)) collected
from 5.3 km altitude near Chesapeake Bay entrance.
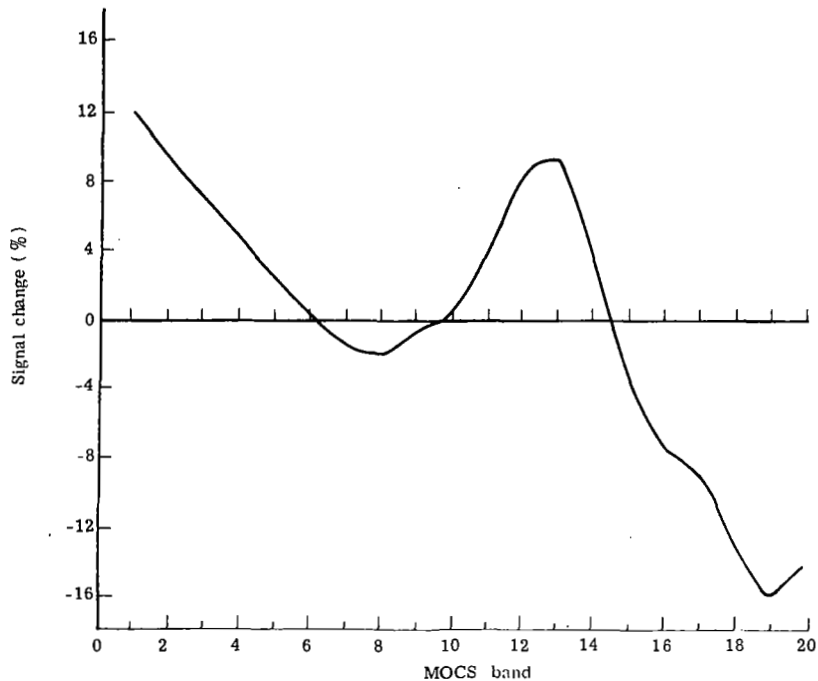
Figure 5.- Difference spectra for data in figure 4 (b).

Region	Date	Solar Elevation	Aircraft Altitude (km)
Norfolk canyon	1/29/74	35°	5.3
New York Bight	4/10/75	43°	5.3
Chesapeake Bay	6/4/75	48°	5.3
New York Bight	7/15/76	30°	5.3
Chesapeake Bay	12/7/78	30°	5.3
Chesapeake Bay	4/30/79	35°	3.2
Midshelf	10/22/80	11°	2.3
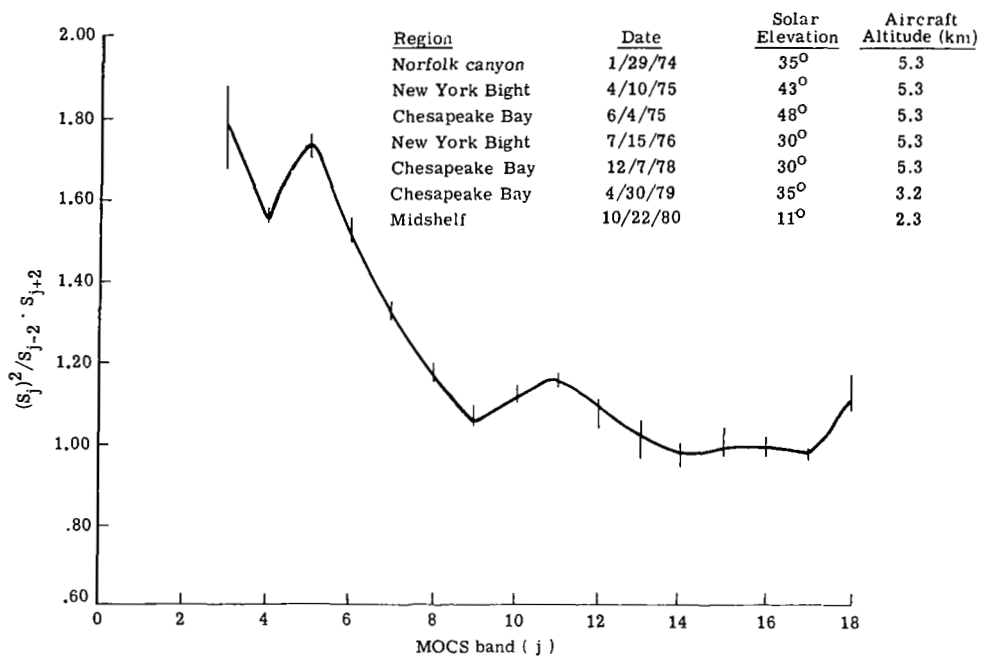
Figure 6.- MOCS inflection ratio spectra for clear water; vertical lines indicate range for samples from listed missions.

$>8\mu g/\ell$ Chlor $\underline{a}$

$<1\,\mu g/\ell$

$H_{j,2}$

MOCS band (j)
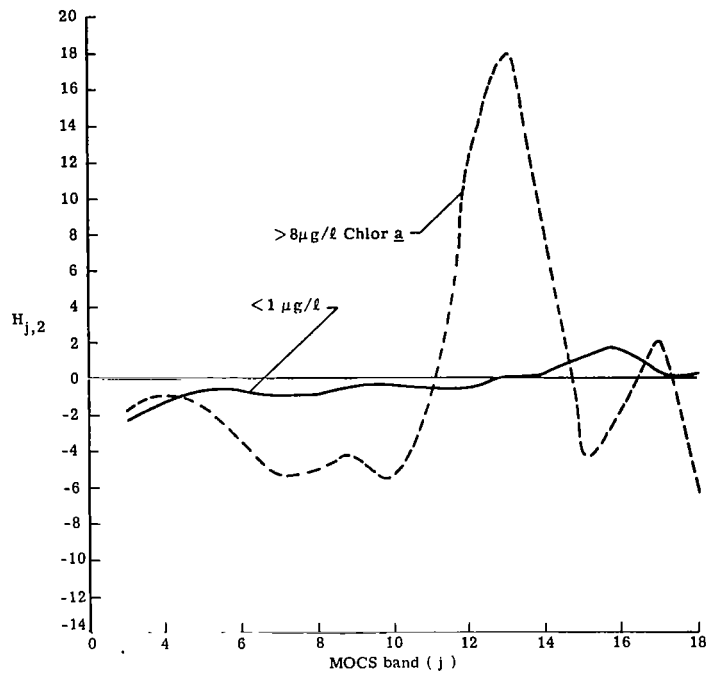
Figure 7.- Inflection ratio spectra for MOCS data in figure 4.

$H_{1,2}$

MOCS band (j)
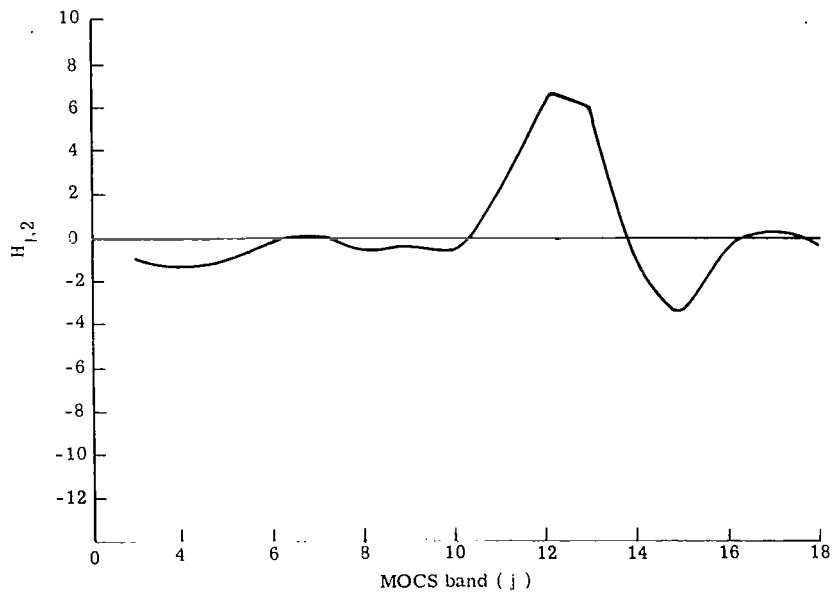
Figure 8.- MOCS inflection ratio spectrum for data collected
near Chesapeake Bay entrance on March 27, 1979.

Washington Canyon

Cape Charles

Norfolk Canyon

James River

Cape Henry

Norfolk

76°

37°

Currituck Sound

75°

74°

Albermarle Sound

36°
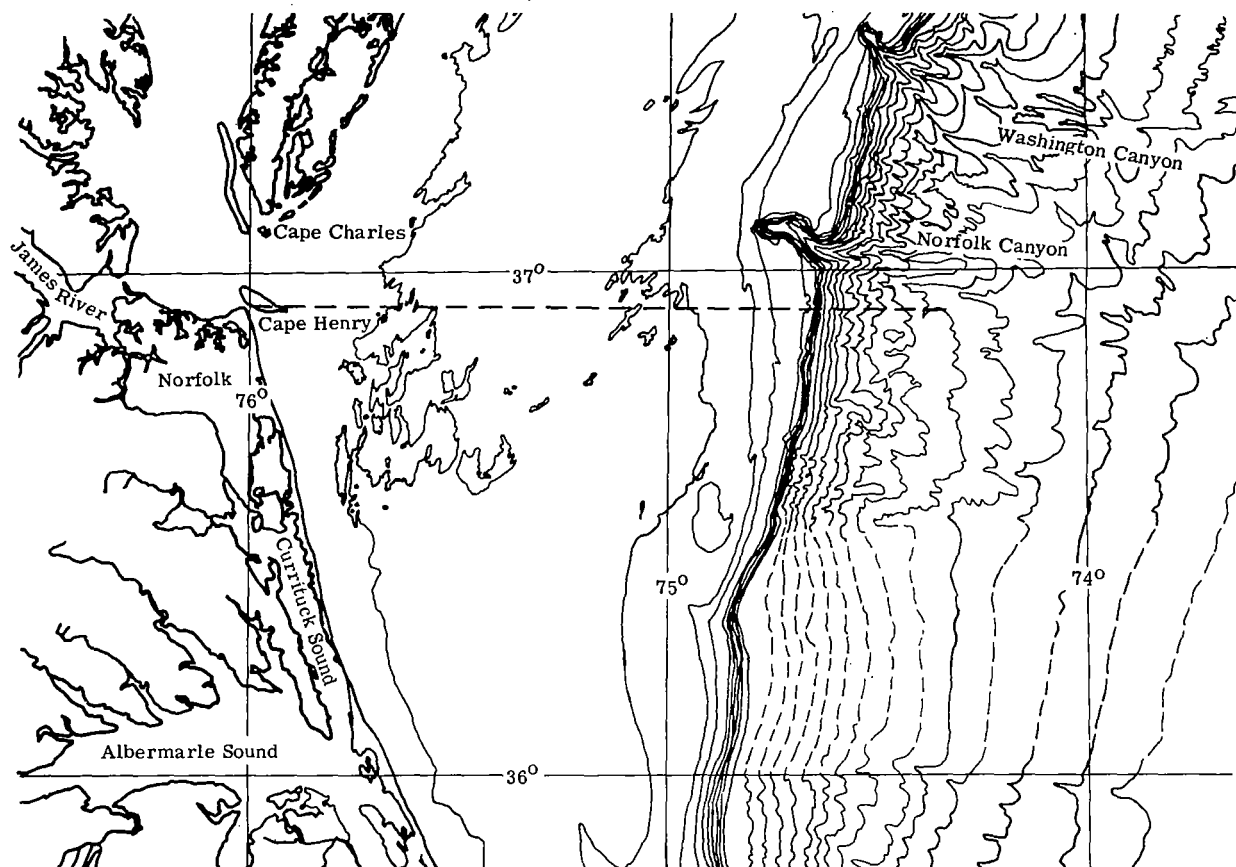
Figure 9.- Track of the Kelez and NASA P-3 on October 21, 1980.

$G_{7,2}$
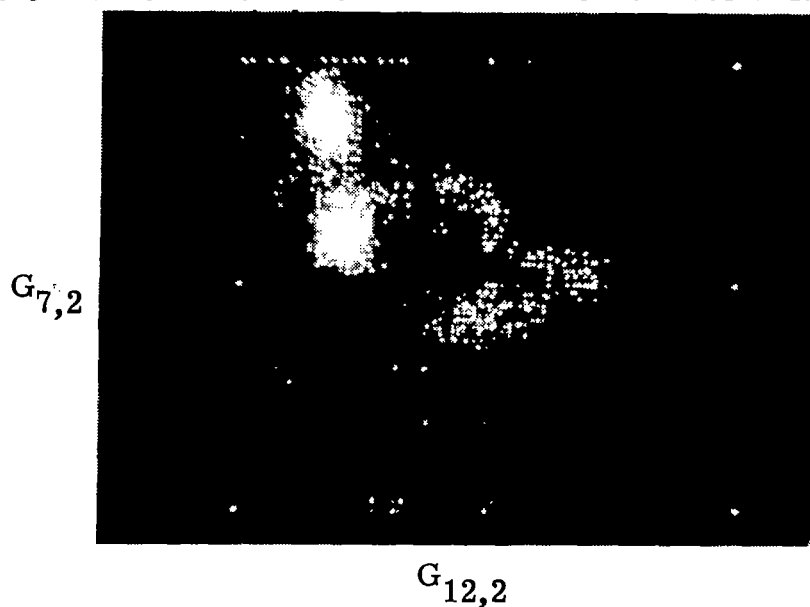
$G_{12,2}$

Figure 10.- Cross plot of $G_{7,2}$ and $G_{12,2}$ for MOCS data
collected on October 21, 1980.
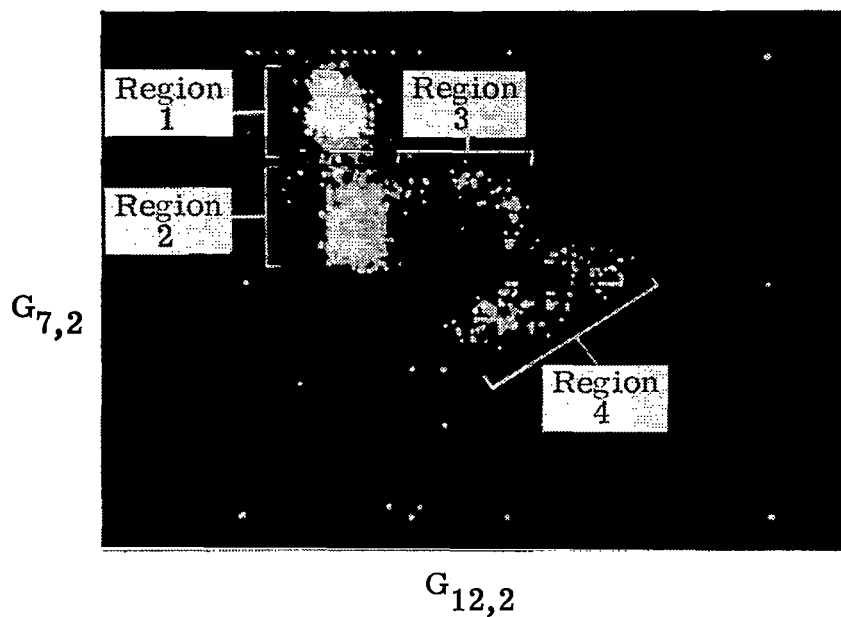
Figure 11.- Same as figure 10 with oceanic regions labeled.
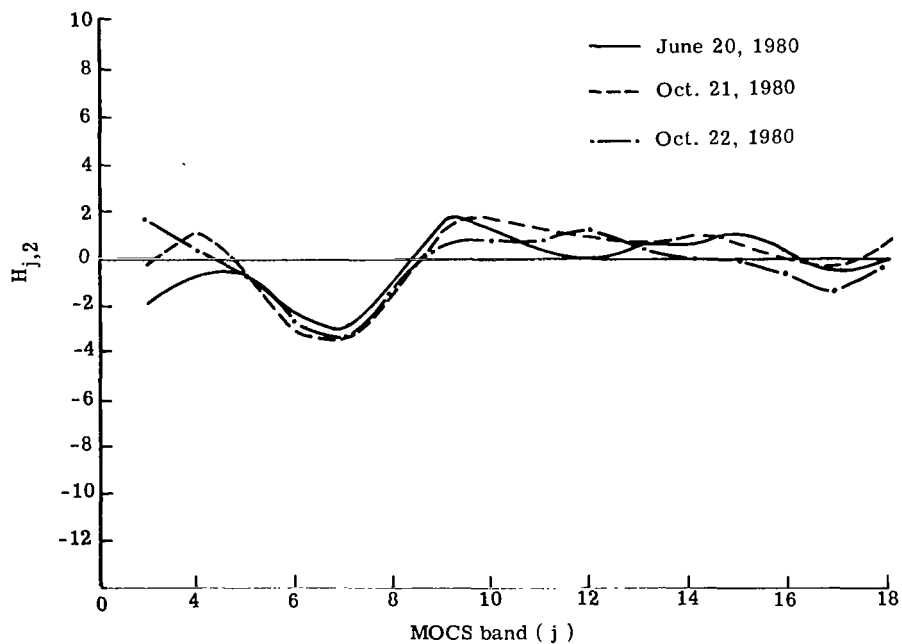
Figure 12.- Inflection ratio spectra for chlorophyll a
(0-2 µg/ℓ) across shelf break.
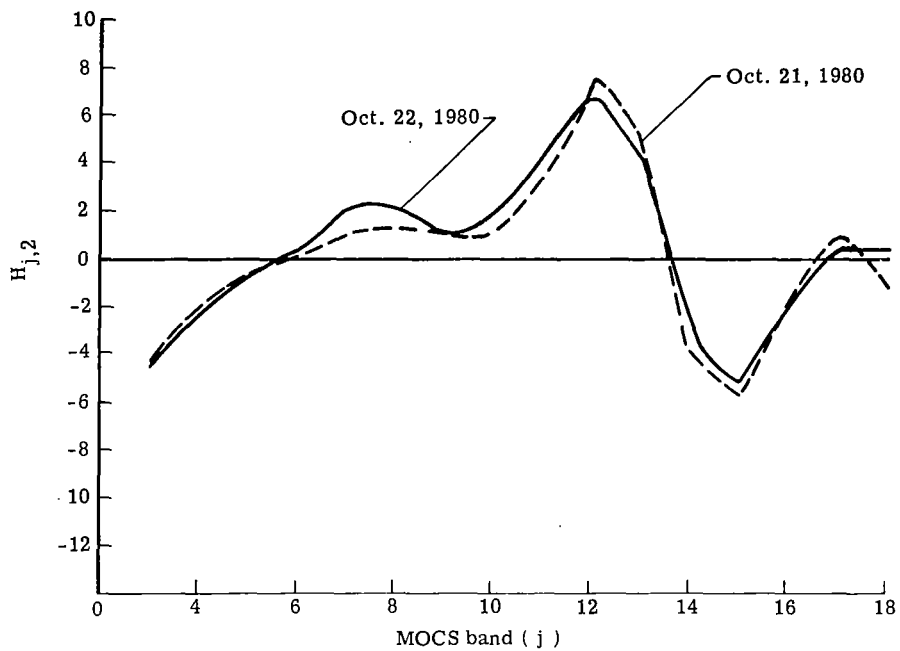
Figure 13.- Inflection ratio spectra between regions 2 and 3.
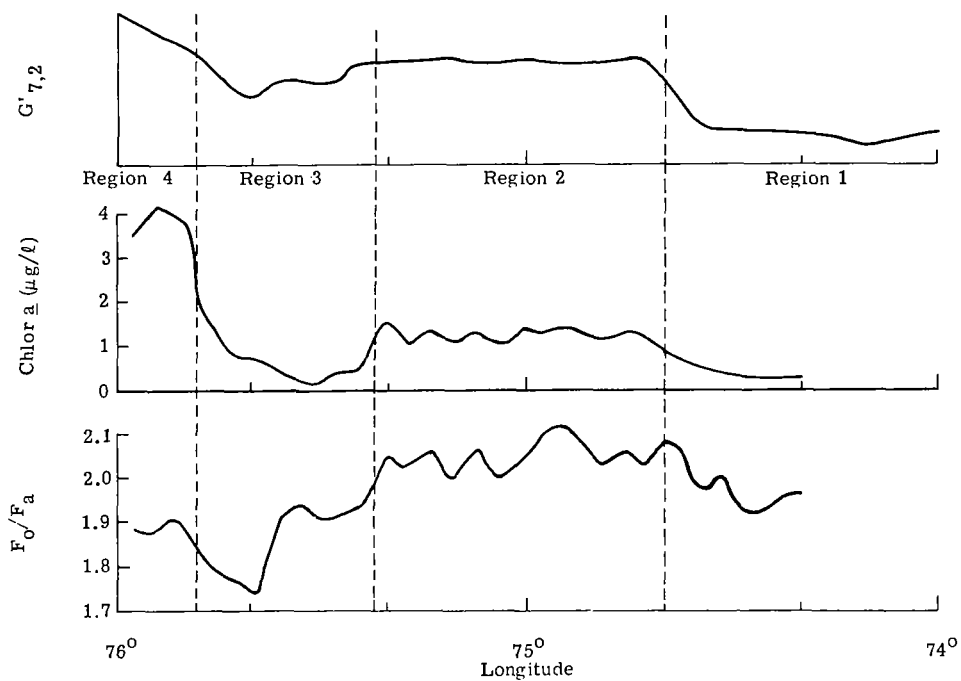
Figure 14.- Sketches of sea truth data and $G_{7,2}$ along flight track on October 21, 1980.
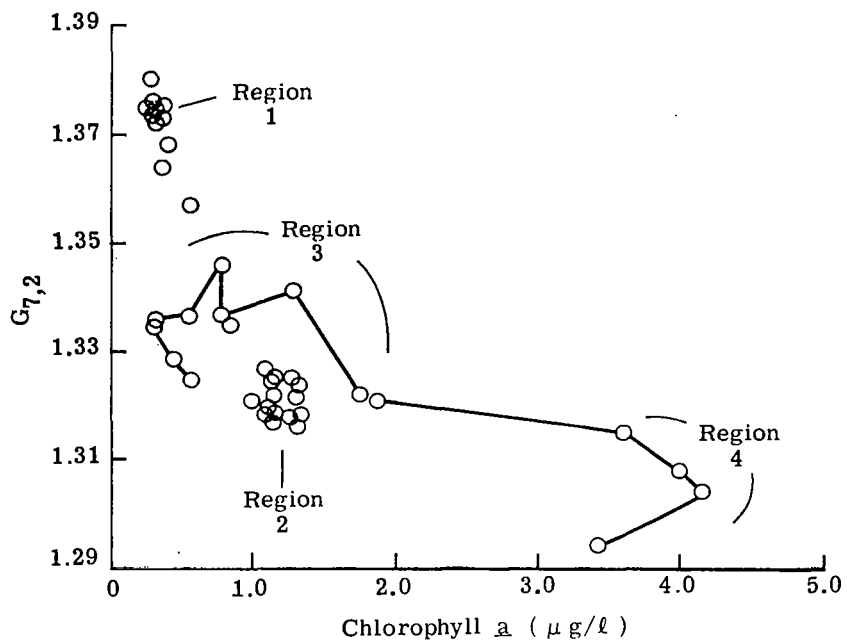
Figure 15.- $G_{7,2}$ versus chlorophyll a for data collected on October 21, 1980. (Lines connect consecutive stations in regions 3 and 4.)
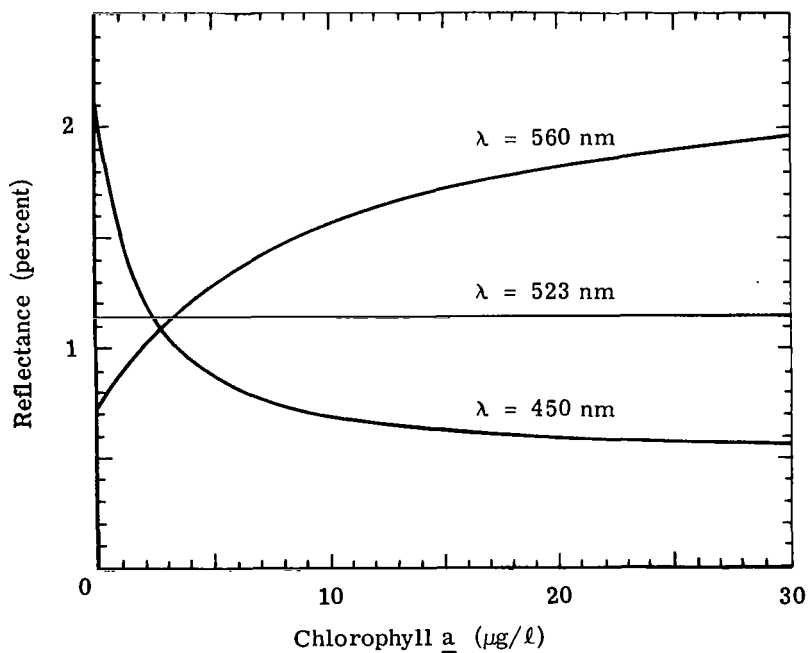
Figure 16.- Reflectance versus chlorophyll a. (From ref. 4).
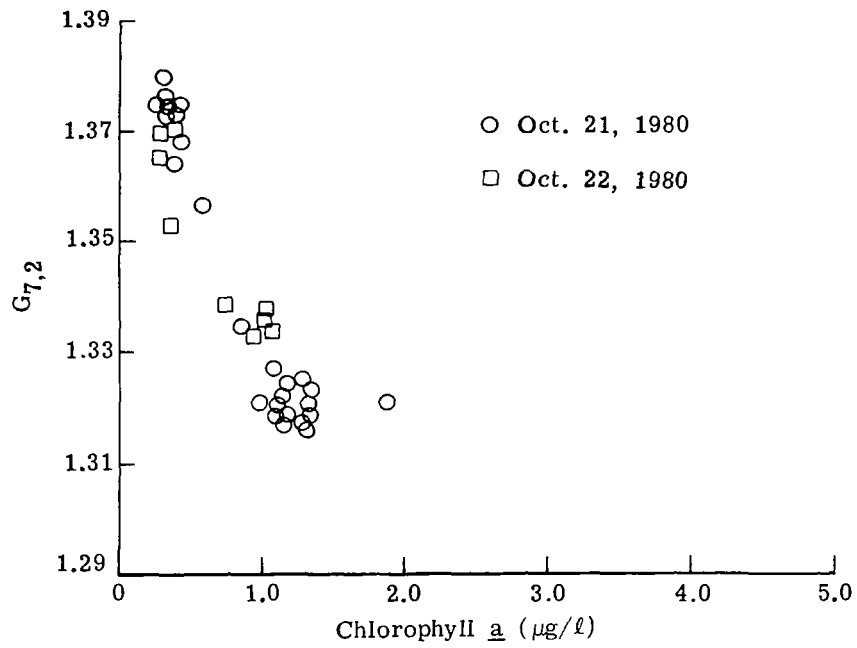
Figure 17.- $G_{7,2}$ versus chlorophyll a for regions 1 and 2.
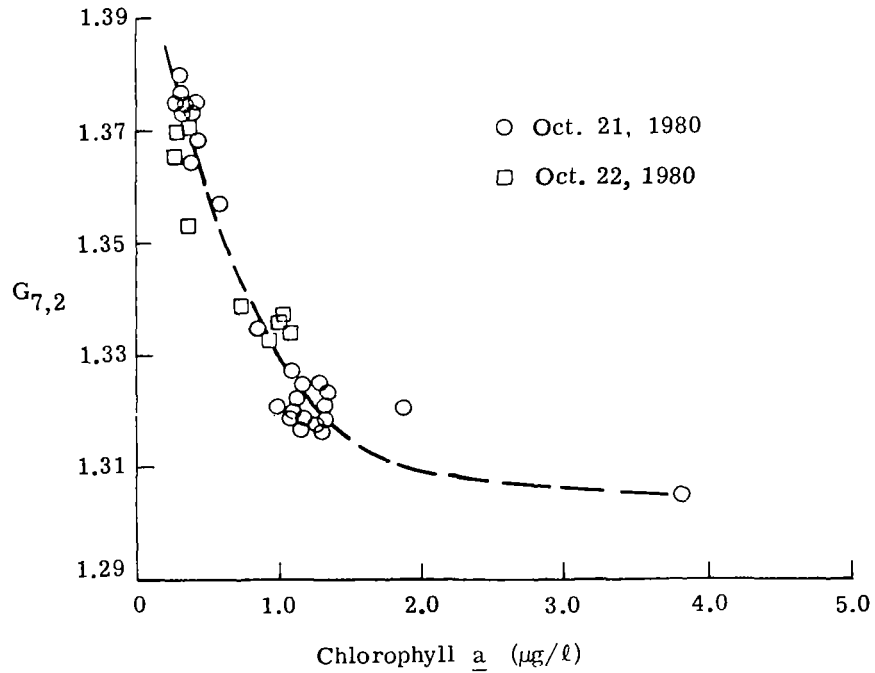
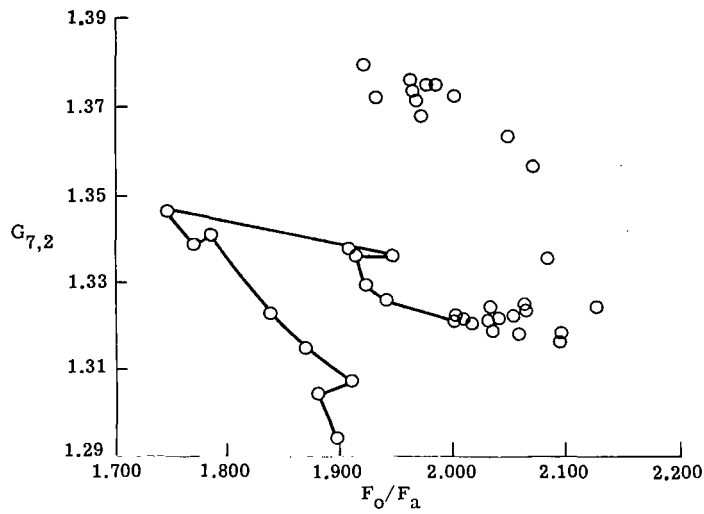Figure 18.- Same as figure 17 with hypothetical curve added.

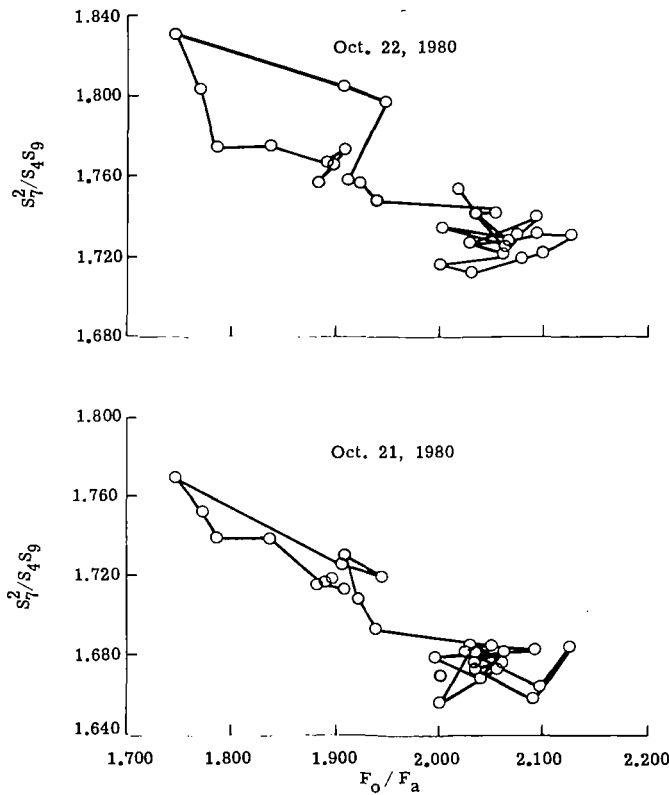Figure 19.- $G_{7,2}$ versus F_o/F_a for data collected on October 21, 1980.

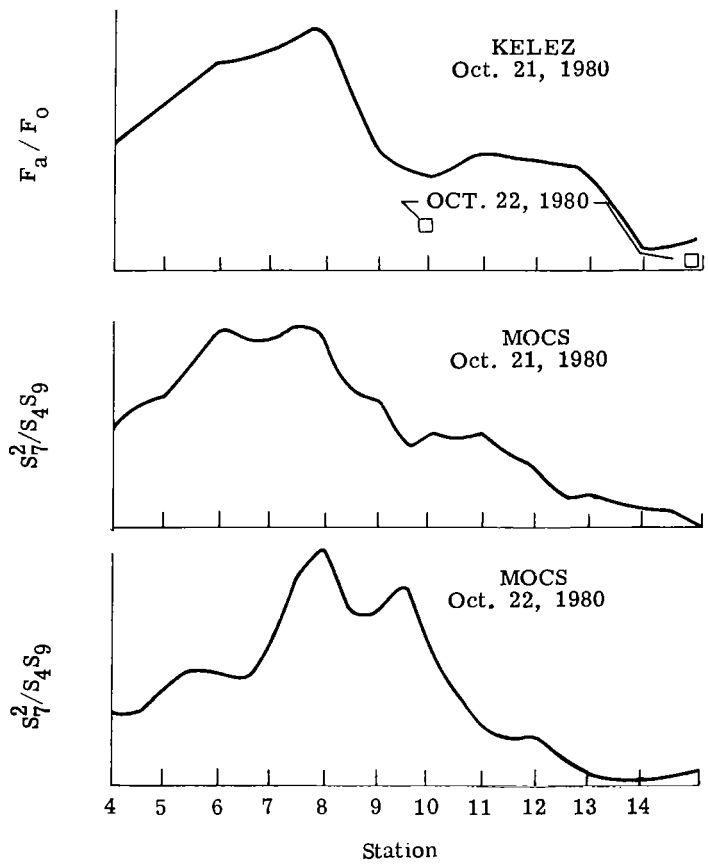Figure 20.- $G_{7,3,2}$ versus F_o/F_a in regions 2, 3, and 4.

Figure 21.- Sketches of F_a/F_o and $G_{7,3,2}$ versus sea truth station in region 3.